

Tilting in the arsenic-induced $c(4 \times 4)$ reconstruction of the GaAs{001} surface

C. Xu, J. S. Burnham, R. M. Braun, S. H. Goss, and N. Winograd

Department of Chemistry, The Pennsylvania State University, 152 Davey Laboratory, University Park, Pennsylvania 16802

(Received 30 September 1994; revised manuscript received 13 March 1995)

The atomic geometry of the As-rich GaAs{001}- $c(4 \times 4)$ surface prepared by molecular-beam epitaxy has been characterized *in situ*. The focus of the study is to determine how excess As affects the structure of the GaAs{001} surface. We report that the second- and third-interlayer spacings are (1.48 ± 0.10) and (1.47 ± 0.10) Å, respectively, in comparison to the bulk spacing of 1.41 Å. Arsenic atoms in the first layer are observed to be dimerized along the $\langle 110 \rangle$ azimuth with a bond length of (2.69 ± 0.10) Å. Furthermore, evidence is presented that is consistent with a structure which contains both untilted and tilted dimers. The tilting is defined by a rotation about the center of the dimer bond by $\pm(4.3^\circ \pm 0.5^\circ)$. These results are based on the desorbed Ga⁺ ion distributions obtained by shadow-cone-enhanced secondary-ion mass spectrometry.

I. INTRODUCTION

Despite the prevalence of Si technology, GaAs is the material of choice for a variety of high-speed devices.¹ The critical optical and electronic properties of current designs incorporating GaAs are established by the layer composition within a nanoscale sandwich. Therefore, the performance of these devices is due in part to the ability to control factors which govern material growth.² For GaAs, the {001} face is most often utilized during fabrication due to the ease of cleaning and the quality of epilayer growth. One of the fascinating aspects of GaAs{001} is the number of structures this surface may possess, each having a characteristic symmetry and stoichiometry.³ A few of these terminations, listed by decreasing surface As concentration, are the $c(4 \times 4)$, (2×4) , (3×1) , (4×6) , and (4×2) . In order to extract the role that the {001} surface plays in the formation of interfaces, an in-depth understanding of the individual reconstructions is necessary. However, the large unit cells and binary composition of the surfaces pose a significant challenge to researchers endeavoring to elucidate the structural properties of semiconductor surfaces.

The GaAs{001}- (2×4) is the most important of these reconstructions and has been studied extensively by a number of structural techniques; however, the geometric arrangement of atoms in the near surface layers is still not completely understood.³⁻⁷ The surface is terminated by 0.5–1.0 ML of As atoms, which are dimerized along the $\langle 1\bar{1}0 \rangle$ crystallographic direction. Moreover, a number of these surface dimers are missing in order to maintain the electronic neutrality of the surface. However, the exact missing dimer structure has not been resolved and a considerable range of dimer bond lengths has been reported $(2.2-2.9 \text{ \AA})$.⁸⁻¹⁰ Despite these ambiguities, the multiple dimer model has been very helpful in formulating mechanistic explanations of growth processes.¹¹

In comparison to the (2×4) reconstruction, structural investigations of other GaAs{001} terminations are limited. These surfaces are important in light of attempts to vary the properties of interfaces with metals by growing

on a structure other than the (2×4) termination. Specifically, the GaAs{001}- $c(4 \times 4)$ structure is important, because of discrepancies concerning the correlation of Schottky barrier heights with As coverage.^{12,13} Such an electronic effect is plausible considering that the work function of the $c(4 \times 4)$ reconstruction has been shown to be a few tenths of an eV less than the (2×4) surface.¹⁴ However, the study of Schottky barrier formation has been complicated by differences in barrier heights formed on $c(4 \times 4)$ surfaces prepared by As decapping.¹⁴ Although the effect of preparation on electronic properties is not clear, As coverage is known to alter metal overlayer ordering.¹⁵ Consequently, detailed structural analyses may aid in understanding how the $c(4 \times 4)$ template influences the properties of overlayers.

Before the Schottky barrier issue erupted five years ago,¹⁶⁻¹⁸ there were only a few structural investigations of the $c(4 \times 4)$ surface. Initial photoemission studies in the early 1980's indicated that the surface is terminated by two layers of As atoms.^{19,20} The atoms in the outermost layer are dimerized, while the second-layer As atoms assume bulklike positions. Moreover, in 1990 three dimer clusters were observed on the $c(4 \times 4)$ surface using scanning tunneling microscopy (STM), thereby confirming the structure shown in Fig. 1.³ This work is supplemented by attempts to pinpoint the surface As concentration and use grazing incidence x-ray diffraction (GIXRD) to determine pertinent structural parameters.^{21,22} The results of the above studies are far from complete as revealed by a recent medium-energy ion scattering study that indicates the second layer of the $c(4 \times 4)$ surface is comprised of almost a 50-50 mixture of As and Ga.⁷

In this study, we present an investigation of the GaAs{001}- $c(4 \times 4)$ surface by shadow-cone-enhanced secondary-ion mass spectrometry (SIMS). This technique has been successfully employed for the analysis of a number of clean and adsorbate covered semiconductor surfaces including the GaAs{001}- (2×4) surface.²³⁻²⁵ The investigation of two GaAs{001} reconstructions by the same technique provides an excellent opportunity to ex-

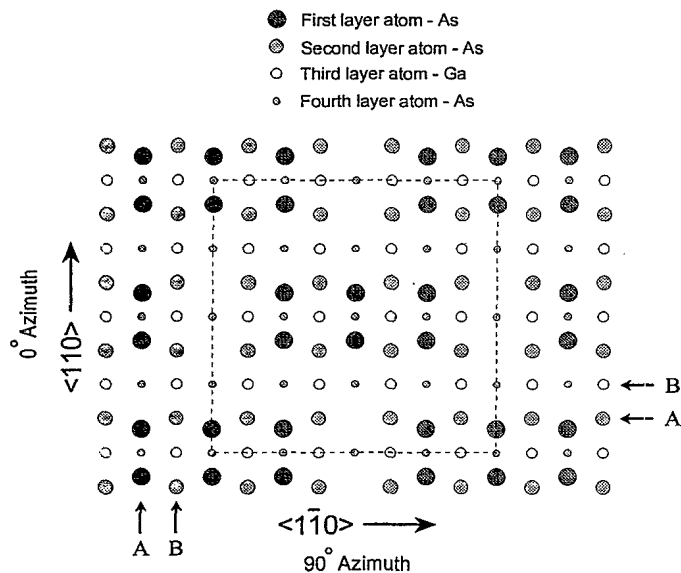


FIG. 1. A schematic for the three dimer model of the $\text{GaAs}\{001\}\text{-}c(4 \times 4)$ surface.

amine the effect of excess As on surface structure. A comparison of these $c(4 \times 4)$ results with structural parameters previously determined for the (2×4) surface indicates that the electronic environment associated with the addition of chemisorbed As mainly affects the arrangement of the outermost As atoms on the surface. The second- and third-interlayer spacings and the As_2 dimer bond distance of the $c(4 \times 4)$ surface are similar to the corresponding spacings on the (2×4) surface. However, we present evidence that in contrast to the (2×4) surface the $c(4 \times 4)$ surface is terminated by a combination of untilted and tilted dimers.

II. EXPERIMENT

A detailed summary of the experimental apparatus and substrate preparation techniques has been presented elsewhere.^{26,27} Briefly, the $\text{GaAs}\{001\}\text{-}c(4 \times 4)$ surfaces were prepared in a Riber 2300 molecular-beam epitaxy (MBE) chamber that is connected to a multitechnique analysis chamber by an ultrahigh vacuum transfer system. Measurements were repeated using three different crystal substrates. A $0.5 \mu\text{m}$ buffer layer was grown on the GaAs wafers prior to each experiment using an 8:1 $[\text{As}_4]:[\text{Ga}]$ flux ratio at a substrate temperature of 850 K. Approximately six experiments were performed on each wafer to check for reproducibility. The growth process was terminated by closing the Ga shutter and the sample was cooled to 620 K under an As_4 flux. At this point, the As shutter was closed and the sample was cooled to 370 K. Once the $c(4 \times 4)$ periodicity was verified using reflection high-energy electron diffraction, the sample was moved to the analysis chamber.

SIMS analysis of the $c(4 \times 4)$ surfaces was initiated by a 3-keV Ar^+ ion beam operated with a total dose less than 1×10^{13} ions/cm². The desorbed secondary Ga^+ ion intensity was measured as a function of the incidence angle of the primary-ion beam. The experimental angular

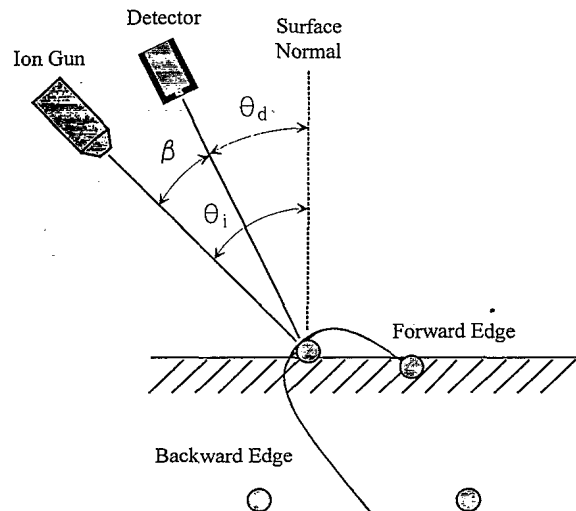


FIG. 2. Parameter definitions for the shadow-cone-enhanced desorption experiment. A schematic of the shadow cone is illustrated with the designations for the forward and backward edge. Note that the presence of a reconstructed surface due to As_2 formation is easily observed through θ_d .

definitions are shown in Fig. 2. The angle of incidence of the primary ion beam θ_i is defined from the surface normal. The azimuthal angle ϕ is defined by rotation about the surface normal at the center of the crystal face and allows us to align a single crystal along a particular crystallographic direction. Each of the three GaAs crystals yielded the same experimental results, within expected error.

III. RESULTS AND DISCUSSION

A. Shadow-cone-enhanced SIMS

The fundamental principle underlying shadow-cone-enhanced SIMS is the shadowing and focusing that occurs during the ion bombardment of an ordered solid. When keV ions impinge on surface atoms their initial trajectory is altered by the repulsive nature of the interaction.²⁸ Consequently, a region of zero flux or shadow is formed behind each surface atom. If all the trajectories are viewed as an ensemble, the edges of this shadowed region possess a significantly increased ion flux.²⁹ As the angle of incidence of the ion beam is varied, the shadow-cone edge will be translated throughout the near surface region. Subsequent interactions of this high-flux edge with lattice atoms leads to enhancements in the secondary-ion intensity.³⁰ With knowledge of the shape of the shadow cone as a function of distance behind the target atom, it is possible to extract surface bonding information from the angular positions of enhanced intensity features by simple triangulation.³¹

This method for determining structural parameters is based on a two-body interaction model.³⁰ The method of extracting bonding information from shadow-cone-enhanced SIMS spectra acquired from the $c(4 \times 4)$ surface is similar to the procedure outlined during the analysis of $\text{GaAs}\{001\}\text{-}(2 \times 4)$ (Ref. 23) and involves a

two-step process. First, the angles at which the high-flux edge of the shadow cone intersects neighboring atoms are calculated for a given surface-structure model using a Cartesian coordinate system. The second step involves directly comparing peak positions calculated from the surface-structure model to experimental peak positions. The atomic positions in the model structure are then adjusted to improve the fit with experimental data. The usefulness of this approach was demonstrated by molecular-dynamics simulations of the sputtering process, which were used as a rigorous basis for understanding the mechanisms of atomic desorption.²³ Since the underlying structure of the (2×4) surface is similar to the $c(4 \times 4)$, the basic desorption mechanisms are not expected to differ. Therefore, an independent molecular-dynamics calculation was not performed for the $c(4 \times 4)$ reconstruction.

In the two-body collision model, the shadow-cone shape of the Ar^+ /surface-atom interactions is determined by incorporating the Molière approximation to the Thomas-Fermi potential in classical scattering formalism.^{29,32} In order to accurately describe the shape of a shadow cone, this potential requires a correction factor for the Firsov screening length, which may be calculated from an empirical expression or determined experimentally. For $\text{GaAs}\{001\}-(2 \times 4)$, the correction factor was experimentally determined to be 0.97, in good agreement with calculation.²³ Since this correction factor depends on the atomic numbers of the interacting species and not on the local electronic structure, the same factor is utilized in this study.

As in the analysis of the (2×4) surface, it is not possible to unambiguously assign all of the features in the spectra. For example, molecular-dynamics simulations indicate that features near $\theta_i = 45^\circ$ are affected by blocking and channeling of the desorbing Ga^+ ions. In order to improve signal-to-noise levels, each of the spectra presented are the sum of a few individual scans. The experimental precision is $\pm 0.5^\circ$, which corresponds to $\pm 0.05 \text{ \AA}$ in most cases; however, we feel that background effects limit the precision in reported bond distances to 0.10 \AA .²³

B. Analysis of the $\text{GaAs}\{001\}-c(4 \times 4)$

The $c(4 \times 4)$ surfaces analyzed in this study are considered to be primarily comprised of three dimer units based on STM and temperature programmed desorption (TPD) measurements of samples prepared in a similar manner.^{3,21} A top view of the three dimer model for the $\text{GaAs}\{001\}-c(4 \times 4)$ surface is shown in Fig. 1. Cross sections of this surface along the $\langle 110 \rangle$ and $\langle 1\bar{1}0 \rangle$ azimuths are shown in Fig. 3 along with the corresponding layer assignments. The atoms are referenced by their row and column positions. These descriptors define which atoms are involved in the shadow-cone process, while the letters refer to the forward and backward edges of the shadow cone, respectively. The dimer atom positions are denoted by a shift (Δ) from the bulk column positions. The shadow-cone-enhanced SIMS spectra for the $c(4 \times 4)$ surface recorded along the $\langle 110 \rangle$ and $\langle 1\bar{1}0 \rangle$ azimuths are

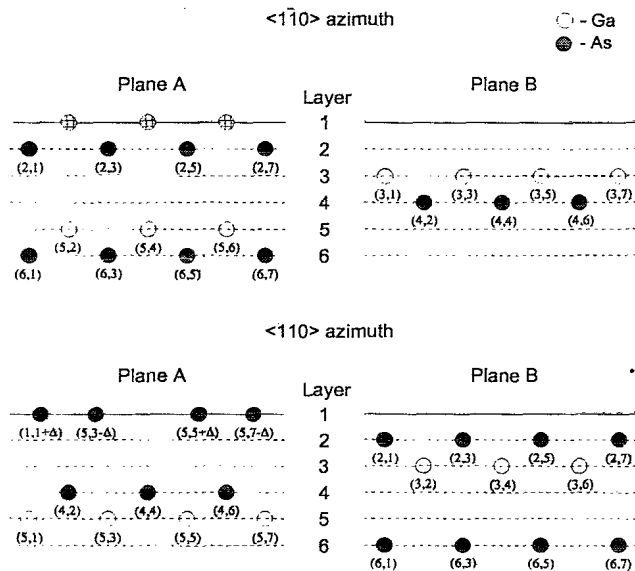


FIG. 3. Side views of the $\text{GaAs}\{001\}-c(4 \times 4)$ surface along the $\langle 1\bar{1}0 \rangle$ and $\langle 110 \rangle$ crystallographic directions. The hatched circles represent As atoms that are shifted out of the plane of the paper by dimerization. The atoms are labeled by row and column descriptors.

shown in Figs. 4 and 5.

The spectrum acquired along the $\langle 1\bar{1}0 \rangle$ azimuth is characterized by two features at $\theta_i = 70.1^\circ$ and $\theta_i = 24.9^\circ$, which arise from the direct interaction of the shadow-cone edge with neighboring atoms. The peak at $\theta_i = 70.1^\circ$ results from two mechanisms. Specifically, the intensity is due to the $F(2,1)(2,3)$ and $F(3,1)(3,3)$ mechanisms that involve an atom focusing flux on a neighboring atom within the same layer. We believe this feature is a good choice for confirming the Firsov screening length correction factor discussed above, because the atoms participating in the mechanism reside in the same layer and are not thought to buckle or laterally reconstruct.³³ Based on the bulk spacing of 4.00 \AA and the correction factor of 0.97, the calculated interaction angles associated with these mechanisms are $\theta_i = 70.0^\circ$ and $\theta_i = 70.1^\circ$, respectively. The calculated angles are not the same, because the second and third layers contain different types of atoms. During this and subsequent calculations, the same factor is used to describe both Ar^+/As and Ar^+/Ga interactions, since individual factors cannot be unambiguously determined. Negligible error is introduced by this approximation, because the shadow-cone shapes for Ar^+/As and Ar^+/Ga interactions are similar, due to the small difference between the atomic numbers of the two atoms (As:33, Ga:31).

Having established the correct shadow-cone shape, we may proceed to the determination of structural parameters. In Fig. 4, an intensity feature is observed at $\theta_i = 24.9^\circ$ that may be used to determine the third-to-fourth-layer separation. The enhanced intensity is attributed to an $F(3,1)(4,2)$ -type interaction, where the incident ion beam is focused by third-layer Ga atoms onto fourth-layer As atoms. Based on this interaction, the spacing between the third and fourth layers is determined

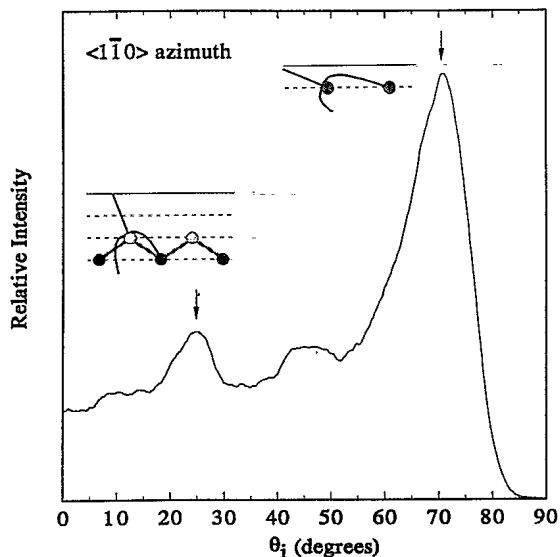


FIG. 4. The relative intensity of 20-eV Ga^+ ions desorbed from the $\text{GaAs}\{001\}$ - $c(4 \times 4)$ surface by 3-keV Ar^+ ion bombardment, plotted as a function of the ion-beam incidence angle (θ_i). The ion beam is parallel to the $\langle 1\bar{1}0 \rangle$ crystal direction.

to be (1.47 ± 0.10) Å. This value is slightly larger than the corresponding interlayer separation of (1.43 ± 0.10) Å for the (2×4) surface. Although the increase is indicative of an expansion, the difference is within experimental error and is not believed to represent a significant change in the interlayer separation.

A further noteworthy observation concerning the spectra recorded along the $\langle 1\bar{1}0 \rangle$ azimuth is that a feature related to surface dimers is not present. This enhanced intensity should appear in the incidence angle range of $\theta_i = 60^\circ$ and $\theta_i = 68^\circ$, based on a reasonable dimer bond length (between 2 and 3 Å). The corresponding spectrum

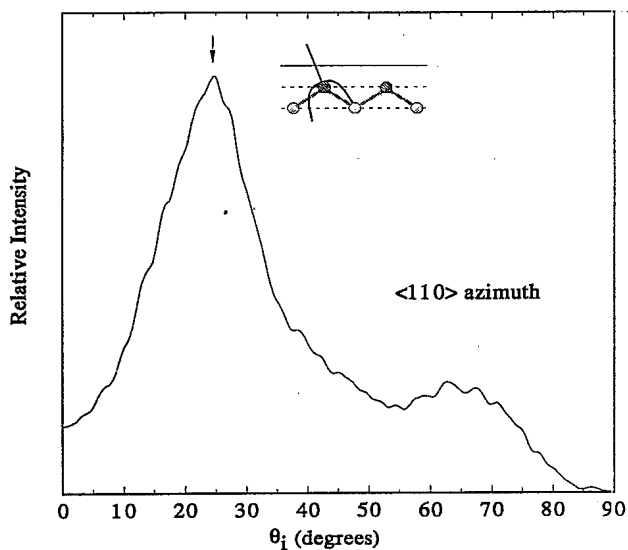


FIG. 5. The relative intensity of 20-eV Ga^+ ions desorbed from the $\text{GaAs}\{001\}$ - $c(4 \times 4)$ surface by 3-keV Ar^+ ion bombardment, plotted as a function of the ion-beam incidence angle (θ_i). The ion beam is parallel to the $\langle 110 \rangle$ crystal direction.

from the $\text{GaAs}\{001\}$ - (2×4) surface clearly exhibits a shoulder at $\theta_i = 63^\circ$ on the side of a peak at $\theta_i = 70.1^\circ$.²³ On the basis of molecular-dynamics simulations, the shoulder is attributed to surface As atoms, which are displaced from their bulk positions along this direction. The fact that atoms are not dimerized along the $\langle 1\bar{1}0 \rangle$ azimuth of the $c(4 \times 4)$ surface is not surprising because the directional bonding of GaAs requires that pairing up in this direction should occur between As atoms in the second layer.

We now consider the spectrum obtained along the $\langle 110 \rangle$ direction. The distribution is dominated by a large feature at $\theta_i = 24.6^\circ$, arising from the $F(2,1)(3,2)$ mechanism. These interactions are characterized by second-layer As atoms focusing incident ion flux onto third-layer Ga atoms. Consequently, the second to third-layer spacing is (1.48 ± 0.10) Å. This value is larger than the second to third-layer spacing of (1.40 ± 0.10) Å for the (2×4) surface and also may represent a slight expansion of the second- to third-layer separation, although the spacing difference is just smaller than the experimental error. An expansion is plausible based on reported changes in the surface electronic structure induced by excess As on the surface.^{14,34,35} Higher-resolution techniques, like surface-extended x-ray-absorption fine structure, might be valuable to further refine this observation.

It would be interesting to be able to estimate the spacing between a first-layer As atom and a second-layer As atom, d_{12} as denoted in Fig. 3. With the present scheme, this measurement has not been possible since the As dimers are shifted out-of-plane and the respective shadow-cone interactions would occur away from the major crystallographic direction. Along $\langle 110 \rangle$, there would be a d_{14} interaction, although this feature was not observed and it would be difficult to deduce the d_{12} value from this value, in any case.

In the high incidence angle portion of the spectrum, four features occurring at $\theta_i = 58.6^\circ$, 62.8° , 67.2° , and 70.2° are observed. The intensity and angle position of these features was identical for each of the three crystals that were studied. The enhanced intensity at $\theta_i = 70.2^\circ$ is attributed to the $F(2,1)(2,3)$ mechanism, which is analogous to the $F(2,1)(2,3)$ and $F(3,1)(3,3)$ in the $\langle 1\bar{1}0 \rangle$ direction. Upon examination of Fig. 1, a second interaction appears to be possible between fourth-layer atoms that are exposed to incident ions. However, the $F(4,2)(4,4)$ mechanism is most likely not contributing to secondary-ion intensity observed in this region, because these atoms are shadowed by first-layer atoms at angles above $\theta_i = 60^\circ$. Therefore, atoms within the second layer are the sole contributors and the distance between the As atoms is determined to be (4.04 ± 0.10) Å, in good agreement with the bulk spacing of 4.00 Å.

The other three features observed in this angular region are related to reconstructions of the adsorbed As atoms. The feature at $\theta_i = 62.8^\circ$ is indicative of As atoms, which are dimerized. This interaction arises from the $F(1,1+\Delta)(1,3-\Delta)$ mechanism and corresponds to an As_2 dimer bond length of (2.69 ± 0.10) Å. The distance is very close to the bond length of 2.73 Å determined for

the As_2 surface dimer in the (2×4) structure. In comparison, GIXRD results indicate that the dimer bond length is $(2.59 \pm 0.06) \text{ \AA}$.²² The difference in these two results may be attributed to the surface model used in the GIXRD study, which was comprised of a mixture of two and three dimer domains. Our results are based on a three dimer model, which is in agreement with recent STM results.³ A slight decrease in the As_2 dimer bond is not unreasonable considering the electronic structure of the $c(4 \times 4)$ and (2×4) surfaces. In the case of the (2×4) structure, the dimerized As atoms are bonded to Ga atoms, which are less electronegative and, therefore, are expected to donate a partial charge to the As. On the other hand, the As_2 dimer atoms on the $c(4 \times 4)$ surface are bonded to As atoms so less charge separation is expected [see Ref. 35 for an in-depth discussion of charge separation on the (2×4) and $c(4 \times 4)$ surfaces]. The result of this difference is that the As_2 dimer atoms on the $c(4 \times 4)$ surface have a weaker interaction with the substrate than those on the 2×4 surface.²¹ Due to this decreased interaction, the dimer bond distance is expected to be smaller on the $c(4 \times 4)$ surface. However, our results indicate that these electronic changes do not significantly affect the As_2 dimer bond length or the inter-layer spacings. In contrast, a more dramatic structural change is observed in the configuration of the surface As atoms.

The appearance of two features at $\theta_i = 58.6^\circ$ and 67.2° on either side of the dimer feature is particularly interesting. Interactions between surface atoms and lower layer atoms are not expected to occur in this angular range. Even when relaxations and reconstructions are considered, there are no lower layer atoms in the vicinity of the shadow-cone edge. The types of mechanisms, which are expected in this region are those involving surface atoms, such as the dimer mechanism $F(1,1+\Delta)(1,3-\Delta)$. If we consider adjusting the positions of the surface As atoms to obtain configurations that will account for these features, there are two possible explanations. One is that there are As dimers on the surface with bond lengths that are less than and greater than 2.66 \AA . However, this model is not probable, because the bond lengths would be 2.23 and 3.39 \AA . Such a wide range of dimer bond lengths has yet to be observed within the same semiconductor surface and would be indicative of very different localized chemical environments.³⁶ Furthermore, 2.23 \AA is close to the 2.1-\AA bond length for the gas phase As_2 dimer.³⁷ A value of this magnitude implies that the electronic environment of the GaAs substrate does not influence the dimer bond.

A second explanation for the peaks on either side of the dimer feature at $\theta_i = 62.8^\circ$ is that some of the dimers on the surface are tilted. The enhanced intensity at $\theta_i = 58.6^\circ$ and $\theta_i = 67.2^\circ$ corresponds to dimers with a bond length of $(2.69 \pm 0.10) \text{ \AA}$ tilted at $\pm(4.3^\circ \pm 0.5^\circ)$. An illustration of the relationship between the tilted dimers and the observed features is presented in Fig. 6. This explanation is based on proposed structures for other semiconductor surfaces. Dimers that are tilted by 7° – 15° have been observed on the $\text{Si}\{001\}$ - (2×1) surface.^{38–41} The cause of the tilting is attributed to the Si dimer

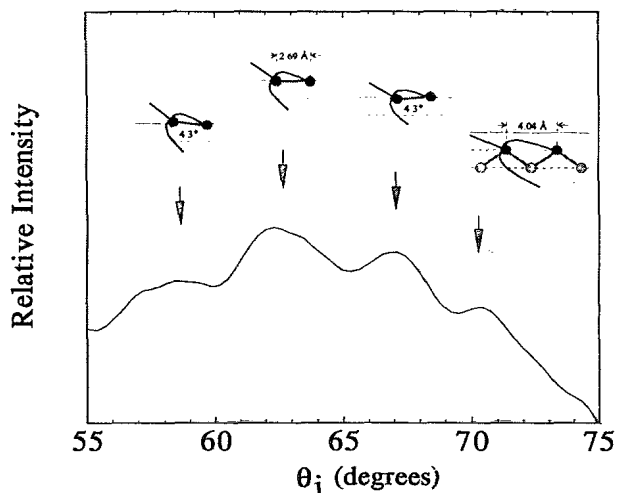


FIG. 6. An expanded view of the intensity between $\theta_i = 55^\circ$ and 75° in the $\langle 110 \rangle$ spectrum. The arrows indicate the enhanced intensity features and the inserts indicate the relative positions of the As atoms involved in the interactions responsible for the features.

atoms having a lone electron in each dangling bond. In order to lower the energy of the surface, one of the dimer atoms assumes an sp^2 configuration and donates an electron to the second atom in the dimer. The resulting configuration does not contain any unpaired electrons.⁴²

For GaAs the same driving force does not exist, although tilted dimer models have been suggested for both the (2×4) and $c(4 \times 4)$ surfaces.^{19,43} Considering the experimental evidence presented to date, recent investigations of the (2×4) surface do not support a tilted dimer model.^{6,8,9} In contrast, the $c(4 \times 4)$ surface is more likely to have tilted dimers than the (2×4) for two reasons. One is the high electron density associated with the excess As that can lead to Coulomb repulsion of the lone pair states. The other factor involves As atoms in the second layer, which do not all possess the same formal charge. The second-layer atoms that have a bond with one first-layer atom have a formal charge of 0, while the atoms bonded to two first-layer atoms have a charge of +1. Despite this reasoning, tilted dimers were not observed in STM and GIXRD studies of the $c(4 \times 4)$ surface.^{3,22} This could be due to a lack of sensitivity to the amount of tilting or differences in the composition of the $c(4 \times 4)$ surfaces. Studies have shown that step edges and defects (including adsorbates) may stabilize tilted dimer structures, although it is not possible to ascertain the role of defects from our measurements.^{41,44}

A further consideration is that the dimers may not be static, but oscillate between the two tilted extremes. This is an interesting quandary, considering the interaction time of keV ions with surface atoms. An energetic ion beam interacts with lattice atoms on a time scale ($\sim 10^{-15}$ sec) that is several orders of magnitude shorter than the period of the oscillations ($\sim 10^{-12}$ sec).⁴⁵ As a result, the incident ions will provide a sampling of atomic positions as a function of time. From a classical viewpoint, the oscillating atoms will spend more time at

TABLE I. A comparison of the bulk terminated GaAs{001}-(1×1) surface structure and results from the shadow-cone-enhanced SIMS analysis of the $c(4\times 4)$ and (2×4) reconstructions.

	As ₂ bond direction	As ₂ bond length (Å)	As ₂ tilt angle (degrees)	d_{23}^a (Å)	d_{34}^a (Å)
(1×1)		4.00		1.42	1.42
$c(4\times 4)$	$\langle 110 \rangle$	2.69 ± 0.10	$\pm(4.3\pm 0.5), 0.0$	1.48 ± 0.10	1.47 ± 0.10
(2×4)	$\langle 1\bar{1}0 \rangle$	2.73 ± 0.10	0.0	1.40 ± 0.10	1.43 ± 0.10

^a d_{23} and d_{34} refer to the second-to-third- and third-to-fourth-layer spacings, respectively.

the turning points, therefore these positions will be statistically weighted. Consequently, we believe the oscillations may broaden the features, but shadow-cone-enhanced SIMS will be sensitive to the tilting. Note that the classical turning points would be very close to the nuclear coordinates associated with the static model. Moreover, at this stage, subtleties associated with the peak widths make it difficult to extract more information from our data using the simple two-body model.

IV. CONCLUSION

We have used shadow-cone-enhanced SIMS to investigate the structure of a GaAs{001}- $c(4\times 4)$ surface prepared by MBE. A synopsis of the results, along with values for the bulk terminated surface, are shown in Table I. The second- and third-interlayer spacings of the $c(4\times 4)$ surface were determined to be (1.48 ± 0.10) Å and (1.47 ± 0.10) Å, respectively. The weak effects of the excess As atoms on these interlayer spacings is evidence that electron density changes are localized in the first two surface layers. Furthermore, the results indicate that the As atoms of the $c(4\times 4)$ surface dimerize along the $\langle 110 \rangle$ direction, in contrast to dimer bonds on the (2×4) surface, which are along the $\langle 1\bar{1}0 \rangle$ direction. The As₂ dimer bond length is determined to be (2.69 ± 0.10) Å, which is similar to the length of (2.73 ± 0.10) Å for the (2×4) surface. Finally, a structural model containing tilted and untilted dimers is proposed. For the three dimer $c(4\times 4)$ structure, there are two plausible arrangements of dimers on the surface. One arrangement in-

volves three types of domains, each containing a single type of dimer (see Fig. 6 for the three types of dimers). A second arrangement is that for each of the three dimer clusters, the outside dimers are tilted in opposite directions and the inside dimer is untilted. Since shadow-cone-enhanced SIMS samples over a large surface area, differentiating the configurations is difficult. However, the technique has proved to be valuable in showing that excess As on the GaAs surface does not dramatically affect the interlayer spacings or the As₂ surface dimer bond length, but is conducive to the formation of buckled As₂ dimers. These measurements are further evidence that the excess electronic charge, associated with the addition of As, is localized in the uppermost layers. This excess surface charge should affect bonding during the initial formation of Schottky barriers, but is not expected to significantly alter the barrier height of thick layers. Recent investigations of the initial stages of Al adsorption on the GaAs{001}-(2×4) indicate a strong interaction between Al and the underlying substrate.²⁴ Current investigations are addressing how excess As influences Al deposition on GaAs{001}- $c(4\times 4)$ surfaces.

ACKNOWLEDGMENTS

The authors would like to thank B. J. Garrison, R. Blumenthal, K. P. Caffey, and W. K. Way for their fruitful discussions. This work was partially supported by funds from the National Science Foundation and the Office of Naval Research.

¹S. Ohr, *Comput. Design* **1994**, 59.

²K. W. Böer, *Survey of Semiconductor Physics* (Reinhold, New York, 1990), and references therein.

³D. K. Biegelsen, R. D. Bringans, J. E. Northrup, and L.-E. Swartz, *Phys. Rev. B* **41**, 5701 (1990).

⁴M. D. Pashley and K. W. Haberem, in *Semiconductor Interfaces at the Subnanometer Scale*, Vol. 243 of *NATO Advanced Study Institute, Series E*, edited by H. W. M. Salemiak and M. D. Pashley (Kluwer, Dordrecht, 1993), p. 63.

⁵M. D. Pashley, K. W. Haberem, W. Friday, J. M. Woodall, and P. D. Kirchner, *Phys. Rev. Lett.* **60**, 2176 (1988).

⁶V. Bressler-Hill, M. Wassermeier, K. Pond, R. Maboudian, G. A. D. Briggs, P. M. Petroff, and W. H. Weinberg, *J. Vac. Sci. Technol. B* **10**, 1881 (1992).

⁷J. Falta, R. M. Tromp, M. Copel, G. D. Petit, and P. D. Kirchner, *Phys. Rev. Lett.* **69**, 3068 (1992).

⁸S. A. Chambers, *Surf. Sci.* **261**, 48 (1992).

⁹H. Xu, T. Hashizume, and T. Sakurai, *Jpn. J. Appl. Phys.* **32**, 1511 (1993).

¹⁰Hua Li and S. Y. Tong, *Surf. Sci.* **282**, 380 (1993).

¹¹H. H. Farrell, J. P. Harbison, and L. D. Peterson, *J. Vac. Sci. Technol. B* **5**, 1482 (1987).

¹²W. I. Wang, *J. Vac. Sci. Technol. B* **1**, 574 (1983).

¹³M. Missous, E. H. Rhoderick, and K. E. Singer, *J. Appl. Phys.* **60**, 2439 (1986).

¹⁴R. Duszak, C. J. Palmstrom, L. T. Florez, Y.-N. Yang, and J. H. Weaver, *J. Vac. Sci. Technol. B* **10**, 1891 (1992).

¹⁵C. J. Kiely and D. Cherns, *Philos. Mag. A* **59**, 1 (1989).

¹⁶R. E. Viturro, S. Chang, J. L. Shaw, C. Mailhot, L. J. Brillson, A. Terrasi, Y. Hwu, G. Margitondo, P. D. Kirchner, and J. M. Woodall, *J. Vac. Sci. Technol. B* **7**, 1007 (1989).

¹⁷S. P. Wilks, J. I. Morris, D. A. Woolf, and R. H. Williams, *J. Vac. Sci. Technol. B* **9**, 2118 (1991).

¹⁸C. J. Spindt, M. Yamada, P. L. Meissner, K. E. Miyano, T.

- Kendelewicz, A. Herrera-Gomez, W. E. Spicer, and A. J. Arko, *Phys. Rev. B* **45**, 11 108 (1992).
- ¹⁹P. K. Larson, J. H. Neave, and B. A. Joyce, *J. Phys. C* **14**, 167 (1981).
- ²⁰P. K. Larson, J. H. Neave, J. F. van der Veen, P. J. Dobson, and B. A. Joyce, *Phys. Rev. B* **27**, 4966 (1983).
- ²¹C. Sasaoka, Y. Kato, and A. Usui, *Surf. Sci. Lett.* **265**, L239 (1992).
- ²²M. Sauvage-Simkin, R. Pinchaux, J. Massies, P. Calverie, N. Jedrecy, J. Bonnet, and I. K. Robinson, *Phys. Rev. Lett.* **62**, 563 (1989).
- ²³C. Xu, K. P. Caffey, J. S. Burnham, S. H. Goss, B. J. Garrison, and N. Winograd, *Phys. Rev. B* **45**, 6776 (1992).
- ²⁴J. S. Burnham, D. E. Sanders, C. Xu, R. M. Braun, S. H. Goss, K. P. Caffey, B. J. Garrison, and N. Winograd (unpublished).
- ²⁵R. Blumenthal, S. K. Donner, J. L. Herman, R. Trehan, K. P. Caffey, E. Furman, N. Winograd, and B. D. Weaver, *J. Vac. Sci. Technol. B* **6**, 1444 (1988).
- ²⁶R. Blumenthal, K. P. Caffey, E. Furman, B. J. Garrison, and N. Winograd, *Phys. Rev. B* **44**, 12 830 (1991).
- ²⁷K. Caffey, R. Blumenthal, J. Burnham, E. Furman, and N. Winograd, *J. Vac. Sci. Technol. B* **9**, 2268 (1991).
- ²⁸E. S. Mashkova and V. A. Molchanov, *Radiat. Eff.* **19**, 29 (1973); **23**, 215 (1974).
- ²⁹A. G. J. de Wit, R. P. N. Bronckers, and J. M. Fluit, *Surf. Sci.* **82**, 177 (1979).
- ³⁰C. C. Chang and N. Winograd, *Phys. Rev. B* **39**, 3467 (1989).
- ³¹R. Smith, D. E. Harrison, Jr., and B. J. Garrison, *Nucl. Instrum. Methods Phys. Res. Sect. B* **46**, 1 (1990).
- ³²D. J. O'Conner and R. J. Macdonald, *Radiat. Eff.* **34**, 247 (1977).
- ³³G.-X. Qian, R. M. Martin, and D. J. Chadi, *Phys. Rev. Lett.* **60**, 1962 (1988).
- ³⁴H. Tsuda and T. Mizutani, *Appl. Phys. Lett.* **60**, 1570 (1992).
- ³⁵W. Chen, M. Dumas, D. Mao, and A. Kahn, *J. Vac. Sci. Technol. B* **10**, 1886 (1992).
- ³⁶G. A. Somarjai, *Introduction to Surface Chemistry and Catalysis* (Wiley, New York, 1994), and references therein.
- ³⁷K. P. Huber and G. Herzberg, *Molecular Spectra and Molecular Structure* (Reinhold, New York, 1979), Vol. 4, p. 38.
- ³⁸R. M. Tromp, R. G. Smeenk, F. W. Saris, and D. J. Chadi, *Surf. Sci.* **133**, 137 (1983).
- ³⁹B. W. Holland, C. B. Duke, and A. Paton, *Surf. Sci.* **140**, L269 (1984).
- ⁴⁰R. M. Tromp, R. J. Hamers, and J. E. Demuth, *Phys. Rev. Lett.* **55**, 1303 (1985).
- ⁴¹R. J. Hamers, R. M. Tromp, and J. E. Demuth, *Phys. Rev. B* **34**, 5343 (1986).
- ⁴²A. Garcia and J. E. Northrup, *Phys. Rev. B* **48**, 17 350 (1993).
- ⁴³D. J. Chadi, C. Tanner, and J. Ihm, *Surf. Sci.* **120**, L425 (1982).
- ⁴⁴T. Hashizume, Y. Hasegawa, I. Kamiya, T. Ide, I. Sumita, S. Hyodo, T. Sakurai, H. Tochiyama, M. Kubota, and Y. Murata, *J. Vac. Sci. Technol. A* **8**, 233 (1990).
- ⁴⁵J. Dabrowski and M. Scheffler, *Appl. Surf. Sci.* **56-58**, 15 (1992).